nature biotechnology

Expression of trehalose-6-phosphate phosphatase in maize ears improves yield in well-watered and drought conditions

Michael L Nuccio[1], Jeff Wu[2], Ron Mowers[2], Hua-Ping Zhou[1], Moez Meghji[2], Lucia F Primavesi[3], Matthew J Paul[3], Xi Chen[1,5], Yan Gao[1], Emdadul Haque[1,5], Shib Sankar Basu[1] & L Mark Lagrimini[4]

Maize, the highest-yielding cereal crop worldwide, is particularly susceptible to drought during its 2- to 3-week flowering period. Many genetic engineering strategies for drought tolerance impinge on plant development, reduce maximum yield potential or do not translate from laboratory conditions to the field. We overexpressed a gene encoding a rice trehalose-6-phosphate phosphatase (TPP) in developing maize ears using a floral promoter. This reduced the concentration of trehalose-6-phosphate (T6P), a sugar signal that regulates growth and development, and increased the concentration of sucrose in ear spikelets. Overexpression of TPP increased both kernel set and harvest index. Field data at several sites and over multiple seasons showed that the engineered trait improved yields from 9% to 49% under non-drought or mild drought conditions, and from 31% to 123% under more severe drought conditions, relative to yields from nontransgenic controls.

Water supply is a universal factor that limits agricultural productivity[1]. For cereals, drought is the most important abiotic stress limiting yield[2]. Most agricultural crop production relies on rainfall during the growing season, so droughts can have potentially catastrophic and unpredictable impacts on crop yields. The most recent widespread drought in the United States, which occurred in 2012, began with dry soils in March and peaked in September, and reduced maize crop yields by an estimated 25% (ref. 3). Current climatic variability is occurring at a time when the annual rate of crop yield improvement is not keeping pace with the projected future demand for food, and is thereby compounding food insecurity[4,5].

Maize is one of the world's most important crops. It is third in production acreage after rice and wheat and first in grain production, yielding ~1 billion tons annually. It is the highest-yielding cereal (by weight) per unit of land area and is grown in regions susceptible to drought including North and South America, China and other parts of Asia, Africa and Europe. Conventional breeding over the past five decades has developed hybrid lines that are less susceptible to water deficit[6], with improvements attributed to reduced anthesis-silking interval, higher tolerance of decreased resource availability, greater biomass accumulation and delayed leaf senescence or 'staygreen'[7]. Consequently, most modern maize cultivars can withstand brief dry spells during early development and the grain-filling period without much impact on yield. However, water deficit during the transition to reproductive development greatly affects yields in all modern hybrids[8]. Even modest water deficits can disrupt photosynthesis[9,10] and carbohydrate (sucrose[11]) supply to developing ears[12–14]. This can reduce kernel set and ultimately yield. Maize ovary viability is also compromised in plants subjected to water deficit during early reproductive development[8,13–15]. In support of this, kernel set is largely preserved when sucrose is infused into the stalks of drought-stressed plants[8,16,17]. Accordingly, improved allocation of sucrose to kernels is one target for potential improvement for maize drought tolerance[18].

Current genetic modification (GM) technology lacks the power to resolve drought tolerance as a single, broadly applicable solution. Each commercial GM trait is based on a single dominant gene. Genetic evidence shows that many genes contribute to drought tolerance, suggesting that more than one transgene may be required to produce a successful GM trait. Furthermore, GM that reduces the impact of abiotic stress can also decrease yield when no stress occurs[19]. An extensive study of several 'candidate drought genes' in rice showed the transgenes tended to reduce yield in unstressed plants[20]. Given the sporadic nature of rainfall in many environments, particularly in North and South America, viable drought-tolerant crops should not incur yield penalty in good years: that is, a GM drought-tolerance trait must have no impact on the maximum yield potential. GM traits based on overexpression of a plant nuclear factor subunit, a bacterial RNA chaperone or ripening-induced proteins, or downregulation of ACC synthases to improve drought tolerance in maize, have produced encouraging results in both the lab and the field[21–24]. GM maize expressing a *Bacillus subtilis* RNA chaperone (CspB) was released to the market in 2013 as Monsanto's Genuity DroughtGard. According to one report, DroughtGard outperformed competitor hybrids by 5 bushels acre^{-1} (51 kg ha^{-1}) (ref. 25). CspB has been shown to possess

[1]Syngenta Crop Protection, LLC., Research Triangle Park, North Carolina, USA. [2]Syngenta Seeds, Inc., Slater, Iowa, USA. [3]Plant Biology and Crop Science, Rothamsted Research, Harpenden, Hertfordshire, UK. [4]Department of Agronomy & Horticulture, University of Nebraska–Lincoln, Lincoln, Nebraska, USA. [5]Present addresses: Syngenta Biotechnology (China) Co., Ltd., Beijing, China (X.C.); Insmed, Bridgewater, New Jersey, USA (E.H.). Correspondence should be addressed to M.L.N. (michael.nuccio@syngenta.com).

Received 23 October 2014; accepted 8 June 2015; published online 6 July 2015; doi:10.1038/nbt.3277

nonspecific RNA binding activity, a requirement to confer drought tolerance; however, the mechanistic basis for its yield effect is not known[22]. These reports demonstrate that GM has the potential to produce drought-tolerance traits, and they address some ways that water deficit limits productivity in growers' fields. They deal with the symptoms caused by drought, however, rather than with the underlying problem of maintaining sucrose flow and its use in reproductive tissue during drought conditions. This is a main cause of yield loss, and addressing it could provide greater protection. Furthermore, assessing drought tolerance in a crop production environment requires resources that are not often available to publicly funded researchers.

Owing to the variability in field environments, studies of drought tolerance need to be conducted in genetic backgrounds suitable for a growing region at multiple sites over multiple years to adequately replicate the results and demonstrate robust efficacy of the GM trait. Trial design that accounts for the irrigation system, addresses the study objective, reveals plot-level data and supports high statistical stringency in the analysis of the field data is necessary to ensure robustness in field data observations. To our knowledge no peer-reviewed study that fulfills these criteria for GM-based drought-tolerant crops has been published.

One regulatory control point known to be involved in drought tolerance, but not yet re-engineered successfully in crops, is the plant trehalose pathway[26]. Notably, the trehalose pathway affects sucrose utilization, one of the drought tolerance targets in maize female florets. Trehalose is a nonreducing glucose disaccharide, and the trehalose biosynthetic pathway consists of T6P synthase, which produces T6P from UDP-glucose and glucose-6-phosphate, and TPP, which produces trehalose from T6P. T6P is a signal of sucrose status[27] and a powerful growth regulator[28] that integrates sucrose utilization with growth and development in relation to environmental conditions. In response to sucrose, T6P regulates gene expression for growth and development through the protein kinase SnRK1, and hence coordinates plant growth and development with sucrose supply[29–31]. SnRK1 and T6P represent a metabolic control point between stress responses and growth processes[27]. Trehalose pathway function depends on the plant tissue and developmental stage[26,32,33]. For example, the maize *RAMOSA3* gene encodes a TPP that determines inflorescence architecture in a highly cell-specific manner[34] through an unknown mechanism. There are many reports of engineering upregulation of the trehalose pathway; initially this was accomplished by increasing expression of TPS and/or TPP to improve drought tolerance in model plants[35–41], rice[42–44] and potato[45] in greenhouse experiments, but these plants were not tested in field trials. All studies to date, with the exception of those involving the expression of genes in chloroplasts[38], have used plants that constitutively express trehalose pathway transgenes to confer drought tolerance. Drought tolerance has been attributed (by correlation only) to the accumulation of small amounts of trehalose in tissues[42] and effects on stomatal opening[41]. However, a mode of action for drought tolerance on the basis of changes in small amounts of trehalose is not known. T6P is known to regulate SnRK1 (ref. 29), and because of the strong and tissue-specific control exerted by T6P through this mechanism[29,33], constitutive overexpression of trehalose metabolism genes results in pleotropic effects[37,46] that are not desirable in crops.

We targeted the growth phase most sensitive to drought in maize with the aim of increasing kernel set at flowering during drought conditions. This was done by linking the promoter of the rice (*Oryza sativa*) transcriptional regulator gene *Mads6* (*MCM1*, *AGAMOUS*, *DEFICIENS* and serum response factor[47]) to a rice TPP gene. *OsMads6* is expressed in the floral meristem, palea and lodicules of young developing flowers and has an essential role in endosperm nutrient accumulation[48,49]. For the first time, to our knowledge, in highly replicated field trials at different sites and during different years, we show here that overexpressing a TPP gene in a specific pattern in female reproductive tissue substantially can increase maize yield under a wide range of water deficit conditions at flowering, from non-drought through mild to severe drought conditions. Thus, targeting trehalose metabolism for crop improvement may have important global implications for food security.

RESULTS

TPP expression strategy

The *OsMads6* regulatory sequence that was used to target rice TPP1 (refs. 50,51) to young ear tissues is shown in **Figure 1a**. The binary vectors in **Figure 1a** and **Supplementary Figure 1a** show the trait cassette, which includes a promoter and a terminator derived from the *OsMads6*[48,49] gene and contains transcribed and nontranscribed regulatory sequences[52]. The *OsMads6* expression cassette is active in several ear node, ear vasculature and ear spikelet (female floret) tissues (**Fig. 1b**). No expression was detected in silk, and this cassette does not produce trait protein in other tissues including leaves, roots and tassels[52]. Several stable, single-copy backbone-free events containing *OsMads6-Tpp1* were produced by *Agrobacterium*-mediated transformation and, of the eight events detected, events 5217 and 5224 were extensively characterized for trait gene function. Western blot analysis confirmed the presence of trait TPP1 protein in events 5217 and 5224, but not in the A188 (nontransgenic, or wild type) control (**Fig. 1c**). No degradation products were detected. Using the purified recombinant rice TPP1 protein standards, we estimated trait protein abundance to be approximately 2 ng per 100 mg (fresh weight) of spikelet tissue. Expression of *OsMads6-Tpp1* in events 5217 and 5224 resulted in >2-fold reduction ($P < 0.0001$) in T6P content of ear spikelet tissue from growth-chamber grown plants in well-watered and drought conditions (**Fig. 2a**). T6P levels in the controls (~47 nmol per g fresh weight) were very close to published values for T6P levels in wheat endosperm (43–119 nmol per g fresh weight)[30]. Sucrose levels increased up to 20% in events 5217 and 5224 (**Fig. 2b**). The reduction in T6P and increase in sucrose were observed in both unstressed and drought-stressed ear spikelets in events 5217 and 5224 compared to wild-type (WT) controls. Trehalose was also measured in these samples. Although there were no changes in trehalose content attributable to the expression of *OsMADS6-Tpp1*, notably, trehalose decreased fivefold in all drought-stressed samples, including the WT controls (**Supplementary Fig. 2a**). Other metabolites, including UDP-glucose (UDPG), sucrose-6-phosphate (S6P) and glucose-6-phosphate (G6P), also decreased under drought conditions, but less so for S6P and G6P in events 5217 and 5224 than for the control plants (**Supplementary Fig. 2a**,**b**). There were small decreases in UDPG and G6P in events 5217 and 5224, respectively, compared to control plants subjected to well watered conditions.

T6P inhibits SnRK1 in plants and crops[27,30], and T6P-dependent regulation of SnRK1 is a potential mechanism for decreased T6P levels when the *OsMAD6-Tpp1* transgene is expressed. SnRK1 activities were measured in ear spikelet extracts with or without T6P in the assay using [^{33}P]ATP and AMARA peptide, a substrate used in AMP-activated protein kinase assays[27,30]. SnRK1 activities in events 5217, 5224 and the control were similar without T6P in the assay. Drought itself decreased SnRK1 activity by approximately twofold in all lines (**Fig. 2c**). When T6P was included in the assays, SnRK1 was clearly inhibited by T6P, suggesting that regulation of SnRK1 activity may

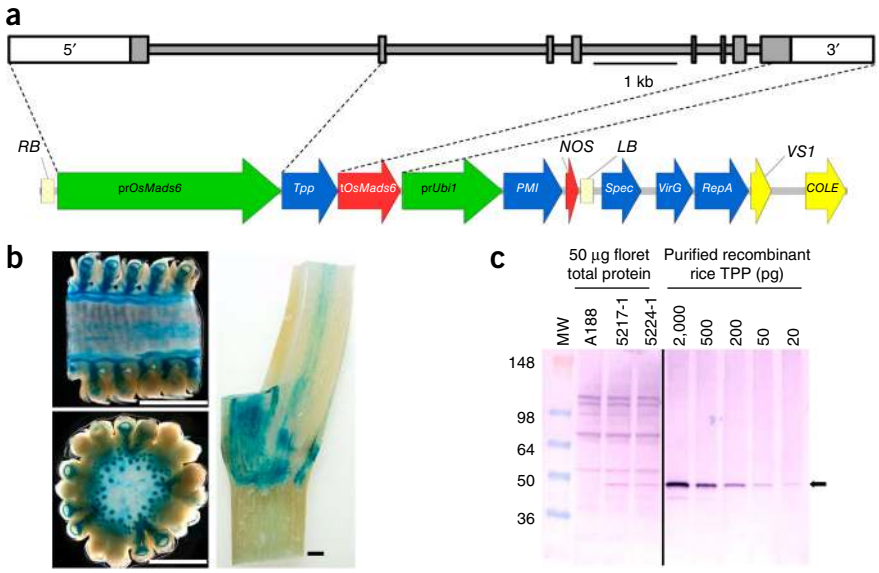

Figure 1 Production of transgenic maize containing the *OsMads6-Tpp1* trait. (**a**) The genomic DNA sequence representing *OsMads6* was annotated by cDNA-gDNA alignment. The promoter is on the right and the terminator is on the left. Open boxes represent nontranscribed sequence, gray is transcript, large gray boxes are exons and narrow gray boxes are introns. These data were used to design trait gene regulatory components. The dashed lines indicate sequence that was incorporated into the *OsMads6-Tpp1* trait gene cassette shown on the linear map of the binary vector used to create the *OsMads6-Tpp1* maize events. Promoters are green, protein-coding sequence is blue and terminators are red. Binary vector components are as indicated in **Supplementary Figure 1**. (**b**) *OsMads6-Gus* expression cassette activity in T1 maize was assessed by histochemical localization of β-glucuronidase (GUS) protein. Left panels show central, longitudinal and cross-sections of the ear, and right panel a stem section taken at the ear node with the ear removed. The *OsMads6* expression cassette is not active, i.e. a histochemical signal is not detected, in other plant tissues including silk, leaf, root and tassel[52]. Samples were harvested 5 d before pollination. Scale bars, 5 mm. (**c**) Detection and quantification of transgenic TPP protein in ear spikelet extracts. Tissue was harvested approximately 5 d before pollination. The 41-kDa rice TPP protein (arrow) was detected with affinity-purified goat antibodies.

be a potential mechanistic basis resulting from changes in T6P levels due to *OsMads6-Tpp1* expression. To test this, we measured the dose response of T6P on SnRK1 activity (**Fig. 2d**) and found 50% inhibition of SnRK1 activity at 50 µM T6P. The estimated tissue concentrations of T6P were 18.8 and 47 µM in transgenic and control plants, respectively; hence T6P levels are in the physiological range to substantially influence *in vivo* SnRK1 activity and provide a mechanistic basis for the effects of *OsMads6-Tpp1* expression.

Field trials of *OsMads6-Tpp1* transgenic maize

Field trials were necessary to test the hypothesis that targeting one part of the trehalose pathway in maize enabled plants to resist the effects of drought during the highly sensitive 2- to 3-week flowering period. Traits that are effective in the laboratory and greenhouse often fail in the field because field conditions vary widely and are difficult to replicate in the laboratory or greenhouse. Our studies incorporated two-row plots with uniform plant densities and uniform genetics (i.e., identical hybrid backgrounds). These were cultivated to produce yields that typically vary by 10–20% of the mean. We conducted field trials on several independent transgenic events to evaluate trait gene efficacy. The trials were replicated at multiple sites, in different years and in germplasm adapted to the trial location, e.g., late-maturing hybrids in California and early-maturing hybrids in Colorado (see **Supplementary Table 1** for details). We took into account the experiences outlined by breeders and the industry when we assessed plant responses to water deficit in the field[53,54]. In all studies we noted that the anthesis-silking interval (the interval between maturation of the male (tassel) and female (ear) reproductive structures) and barrenness (the number of plants without an ear) did not vary between the *OsMads6-Tpp1* events and the controls.

OsMads6-Tpp1 increases yield in the field

In the first stage of field assessment, field variability was addressed by locating plots that contained control plants either adjacent to (sharing a border) or near to (within three plots or ~6 m) transgenic plots (for plot locations see **Supplementary Fig. 3**). *OsMads6-Tpp1* increased yields in both the water-deficit and well-watered (unstressed) treatment blocks (**Fig. 3a**). Replicate blocks were positioned at increasing

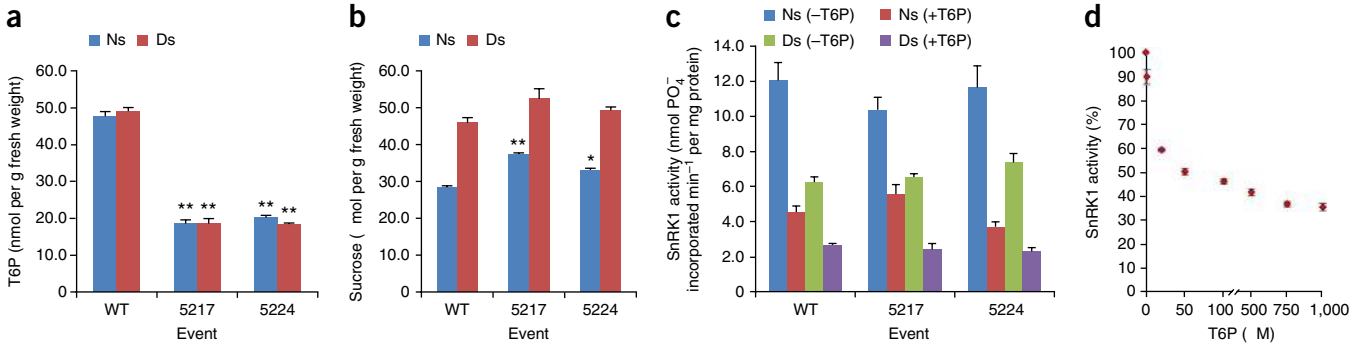

Figure 2 Metabolic and biochemical characterization of *OsMads6-Tpp1* ear spikelets. (**a**–**c**) Levels of T6P (**a**), sucrose (**b**) and SnRK1 activity ± 1 mM T6P (**c**) in spikelets harvested 5 d before pollination. Samples are from unstressed (ns) and drought-stressed (ds) plants. (**d**) T6P dose response on SnRK1 activity in spikelets harvested 5 d before pollination. For **a**,**b**, $n = 4$ for unstressed plants; $n = 5$ for drought-stressed plants. For **c**,**d**, $n = 3$. Data are mean ± s.e.m., $^{*}P < 0.05$, $^{**}P < 0.01$. Computed P values for each comparison are tabulated in **Supplementary Figure 2c**. WT, wild type.

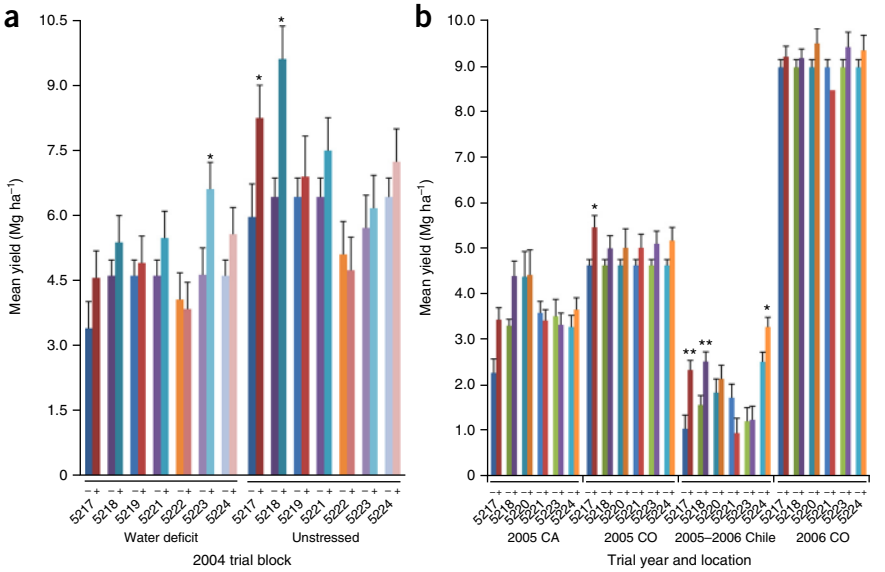

Figure 3 Field performance summaries for several *OsMads6-Tpp1* events. Transgenic events were cultivated in managed stress environments (MSE) in which the water supply was controlled to impose a water deficit during the 3-week flowering period; otherwise the water supply was not limiting. (**a**) The mean plot yields from a 2004 trial in California using adjacent replicate plots. This trial included both water deficit and unstressed blocks. Details are presented in **Supplementary Table 2**. $n = 3$. (**b**) The mean plot yields for several trials conducted over a 2-year evaluation period in California, Colorado and Chile. Plants were cultivated in two-row plots. Yield data are adjusted to 15.5% grain moisture. Data shown are for the transgenic (+) and control (–) material and are the mean ± s.e.m.; $n = 8$–12 (2005 CA); $n = 9$ (2005 CO); $n = 8$–16 (2006 CO); $n = 10$–20 (2005–2006 Chile). Statistically significant linear contrasts of each transgenic to its control are denoted * ($P < 0.05$) and ** ($P < 0.01$).

distances from the water source. As expected, replicate 3 (the furthest from the source in ranges 8–9) received the least water in both the well-watered and water-deficit treatment blocks (**Supplementary Fig. 3**). Water deficit reduced yield by 47%. **Figure 3a** and **Supplementary Table 2** illustrate a consistent yield benefit in transgenic events. Trait performance varied between replicates and events and only event 5222 appeared ineffective. Event 5223 had a statistically significant positive trait performance in the water-deficit treatment block. The six independent transgenic events demonstrated an average yield benefit ranging from 0.30–2.0 Mg ha^{-1} in the water-deficit treatment block.

The well-watered treatment block was not completely devoid of water stress because this trial relied on furrow irrigation (which does not ensure equal water distribution to each replicate). Yields were highest in replicate 1, which is closest to the water source, and lowest in replicate 3, which is furthest from the water source. This may explain the estimated 0.47–3.2 Mg ha^{-1} yield benefit with *OsMads6-Tpp1* in this block. Yield advantages for events 5217 and 5218 were 2.3 and 3.2 Mg ha^{-1}, respectively, compared to their respective controls (**Supplementary Table 1**).

This study also compared yields between trait-positive and corresponding null siblings (controls) for three events. Event 5222 was not statistically different from its corresponding null. However, events 5217 and 5223 showed that yield preservation consistently segregated with the trait gene. This genetic evidence, together with data from several independent events, demonstrates that the *OsMads6-Tpp1* trait gene provides considerable yield benefit under field conditions.

Yield increases consistent over time

OsMads6-Tpp1 events were evaluated in four additional field trials over a two-year period. During that time furrow irrigation was replaced with drip irrigation. The water-management program was made dependent on soil composition, soil moisture and evapotranspiration to more precisely control water deficits. In addition, plot replicates were increased from 3 to ~8 per event and trial design to maximize statistical power was adopted. In some trials each transgenic event plot had a null segregant control plot for each replicate, whereas in other trials the null segregant plots were replaced with WT control plots distributed throughout the field. This enabled more replicates for both transgenic and control plots. The number of replicates was determined using the observed variation in each field and the calculated power required to detect a 10% difference in yield at the $P < 0.10$ confidence level. This resulted in a robust platform to impose water deficits that limited yields to 40–60% of typical yields through deficit irrigation during reproductive development. These improvements further increased trial stringency. During this period events 5219 and 5222 were dropped because they lacked trait performance, and event 5220 was added because it required more time to produce hybrid seed for field trials. The objective of this work was to compare plot yields between transgenic events and controls. We did not observe any relationship between the hybrid genetic background and trait performance.

Data for six independent events tested during this period are summarized in **Figure 3b**. Average differences between transgenics and controls were computed for five drought-stress environments (2004 and 2005 California, 2005 and 2006 Colorado, and 2005–2006 Chile) are 0.83, 0.50, 0.53, 0.21 and 0.43 Mg ha^{-1}, respectively. Each of these environments had a statistically significant difference ($P < 0.05$) except for the one with the least stress (2006 Colorado). The (transgenic – control) differences were averaged (weighting each stress environment equally) and the contrast was tested with Student's *t*-test[55]. The *OsMads6-Tpp1* trait provided a statistically significant +0.50 Mg ha^{-1} average advantage (+8.0 bushel acre^{-1}, $P < 0.0001$) for these five environments. This is an average 10.6% advantage over controls.

The data in **Figure 3** and **Supplementary Table 2** show that each trial produced a unique outcome in terms of drought-induced yield reduction. Typical yield for the germplasm used in these studies ranged from 8.5–9.1 Mg ha^{-1} in well watered conditions. Events 5217, 5218, 5224 and, to a lesser degree, 5220 preserved yield in all studies. Event 5223 tended to preserve yield but not in all studies. Proof of concept for a GM-based drought improvement trait requires that trait performance be evident in multiple trials at multiple locations conducted over multiple years. These data also addressed the two most important hallmarks for proof of concept: yield preservation attributable to *OsMads6-Tpp1* was observed in several independent transgenic events, and the yield preservation phenotype segregated with the transgene. **Figure 4** summarizes the effect of *OsMads6-Tpp1* over the entire study, incorporating data from **Figure 3a**,**b** and **Supplementary Tables 2** and **3**, and is presented as percentage yield benefit of the transgenics compared to their respective controls. The *OsMads6-Tpp1* trait was most effective in high-stress situations,

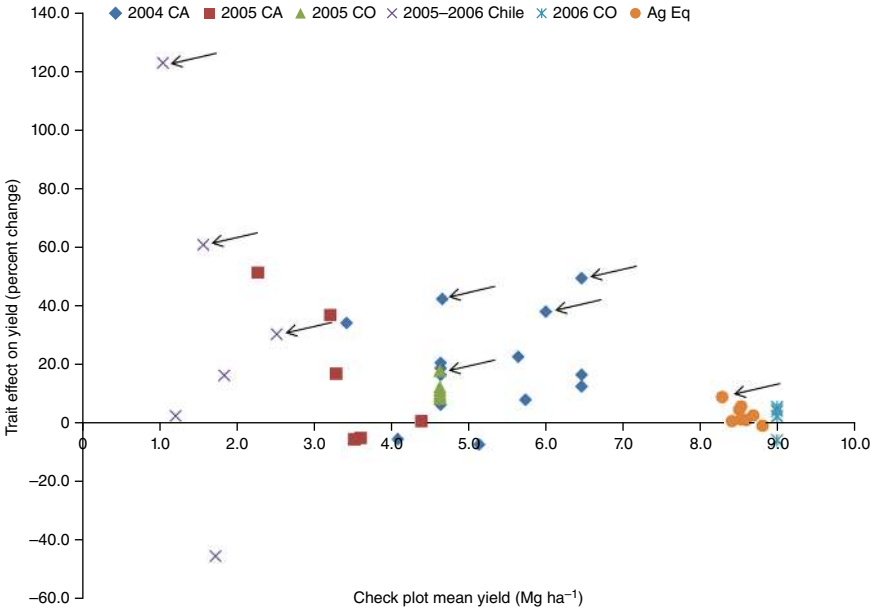

Figure 4 Change in field trial yield outcome due to the *OsMads6-Tpp1* trait. The trait effect is the difference between mean transgenic yield and mean control yield data for each event, and is plotted as a percent of the mean control yield. Each data point represents one event in each trial. The data are from **Figure 3a**,**b** and **Supplementary Tables 2** and **3**. Ag Eq is Agronomic Equivalence, a field study that represents typical grower environments. The arrows indicate statistically significant *OsMads6-Tpp1* effects at $P \leq 0.05$.

in which yield was reduced by ~80%. Nevertheless yield benefits were achieved at all levels of water availability, with statistically significant increases ($P \leq 0.05$) from 9% and 49% where yield loss caused by drought was between 0% and 50%, or between 31% and 123% where drought was more severe. The maize *ramosa3* mutation inactivates a TPP that is specifically expressed in ear spikelet primordia and alters ear morphology[34]. This suggests that *OsMads6-Tpp1* might alter ear appearance as *OsMads6* promoter expression may overlap with *RAMOSA3* expression. Throughout these studies the *OsMads6-Tpp1* trait had no obvious impact on plant or ear morphology; the transgenic and control plants were indistinguishable in this regard.

OsMads6-Tpp1 has no yield penalty

Many transgenes that improve plant response to water deficit do so by slowing growth or reducing productivity, an effect commonly referred to as yield drag. To determine whether *OsMads6-Tpp1* contributed to yield drag, we conducted agronomic equivalency (Ag Eq) trials. These trials are designed and managed to reflect typical grower conditions in several locations throughout the US corn belt. Conditions included plant density, fertilizer use and pest management. The trial design was similar to that described for managed stress environment (MSE) trials, except that the water supply was not actively managed. The Ag Eq trials are used to assess standard yield for new GM traits. Water deficit was not a factor in these trials. Hybrids were cultivated in three early- and six late-maturity environments throughout the North American Midwest during the 2004–2006 growing seasons. Data in **Supplementary Table 3** show that the *OsMads6-Tpp1* trait had no yield penalty, but instead conferred some yield benefit when there was no drought. Orthogonal contrasts of transgenic hybrids versus their null counterparts, after an analysis of variance, resulted in only event 5217 yielding statistically significantly more grain, with other transgenic hybrids also producing more grain than their null counterparts, although the differences were not statistically different.

Yield increases kernels and harvest index

To identify yield components associated with the *OsMads6-Tpp1* trait, events were analyzed for drought response in a greenhouse over a two-year period. Hybrids of eight independent events and their corresponding null segregants (controls) were either well watered throughout development or subject to water deficit during the 3-week flowering period. The water deficit was designed to reduce yield by 50%. **Table 1** shows that transgenics produced more kernels per plant in both

Table 1 ***OsMads6-Tpp1*** **increases kernel set and harvest index in greenhouse studies**

	2005								2006							
	Well-watered block				Water-deficit block				Well-watered block				Water-deficit block			
Event	*N*	Kernels per plant	Shoot dry weight (g)	Harvest index	*N*	Kernels per plant	Shoot dry weight (g)	Harvest index	*N*	Kernels per plant	Shoot dry weight (g)	Harvest index	*N*	Kernels per plant	Shoot dry weight (g)	Harvest index
5217+	3	277*	162	0.319*	3	92	137	0.117	3	306	139	0.339	4	55	173	0.058
5217–	3	120	166	0.155	3	63	136	0.075	3	201	152	0.245	4	26	162	0.030
5218+									3	377*	141	0.373	4	51	175	0.049
5218–									3	245	146	0.277	4	37	168	0.040
5220+									3	345	131	0.369	4	88	165	0.094
5220–									3	225	138	0.273	4	82	164	0.083
5221+	3	197	172*	0.235	3	106*	135	0.138								
5221–	3	239	146	0.300	3	64	136	0.091								
5223+	3	199	199*	0.198	3	152*	145	0.163*	3	247	163	0.260	4	52	180	0.053
5223–	3	209	154	0.264	3	83	144	0.091	3	317	146	0.338	4	34	184	0.044
5224+	3	278	174	0.308	3	56	160*	0.069								
5224–	3	223	168	0.267	3	28	148	0.036								
L.S.D.		96	12	0.088		41	11	0.052		129	15	0.111		54	14	0.052

Results from experiments conducted during consecutive years in Slater, Iowa, USA, showing kernel set and harvest index components that make up yield differences between *OsMads6-Tpp1*–trait positive and controls. *N* is the number of plants, shoot dry weight is the above soil plant mass and harvest index is the kernel weight divided by the above-ground biomass. L.S.D. is least significant difference calculated by analysis of variance as described in the Online Methods. *Indicates a statistically significant difference between transgenic (+) and control (–) plants at $P = 0.05$.

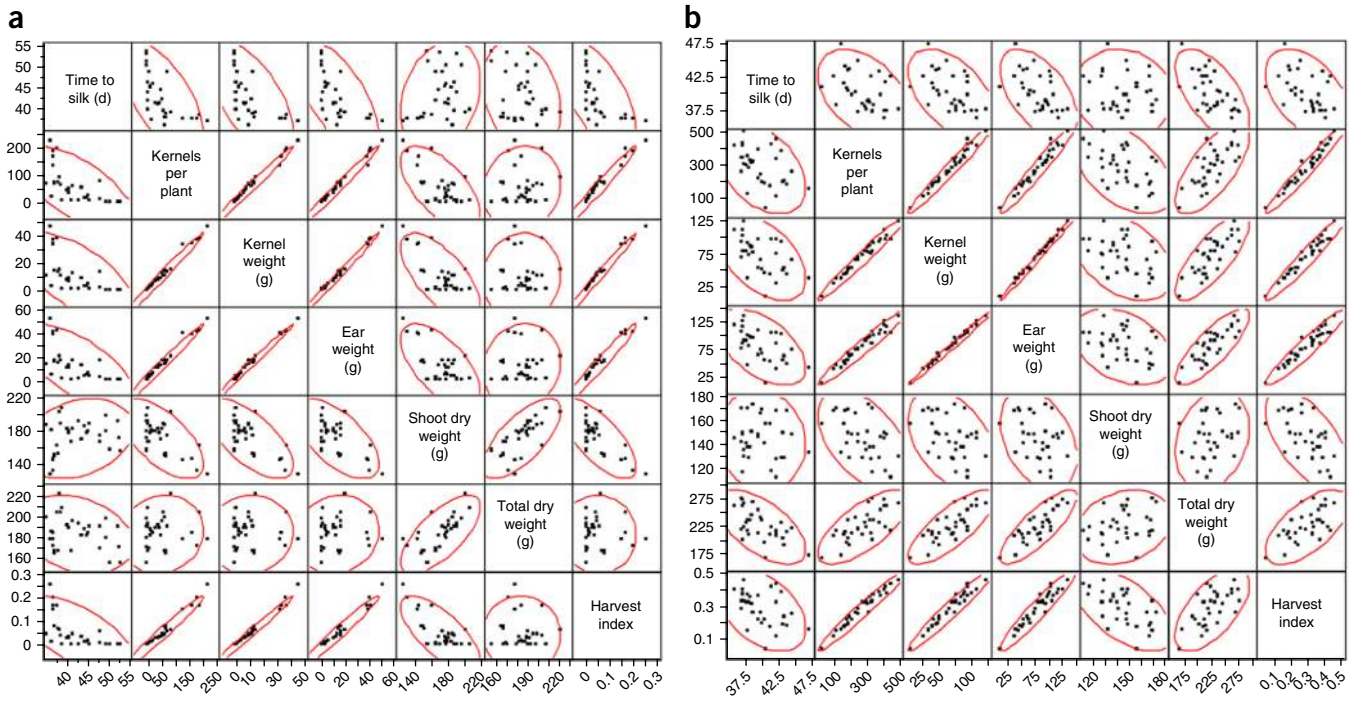

Figure 5 Correlation analysis of trait components for *OsMads6-Tpp1* events in the 2006 greenhouse study. (**a**,**b**) Data for each trait component are plotted as a function of the other trait components from plants in the water-deficit treatment block (**a**) and the well-watered treatment block (**b**). Each plot represents all plants in the treatment block. Units are: time to silk, days; kernels per plant, number of kernels; kernel weight, g per plant; ear weight, g per plant; shoot dry weight, g; total dry weight, g; harvest index, (kernel weight)/(above-ground biomass). The axis labels are in the diagonal boxes in each panel. These data are summarized in **Table 1** and **Supplementary Tables 6** and **7**.

blocks, particularly in the water-deficit block. Here the differences between transgenics and controls varied from 6–69 kernels per plant, and were statistically significant ($P = 0.05$) for events 5221 and 5223 in the 2005 study. In the well-watered blocks, event 5217 in the 2005 study and event 5218 in the 2006 study produced significantly more kernels per plant ($P = 0.05$). Because shoot dry weight was generally stable, increased kernels per plant positively influenced harvest index, particularly in the water-deficit blocks. **Supplementary Tables 4** and **5** show that transgenics in the 2005 study had more biomass per plant relative to controls. *OsMads6-Tpp1* decreased the root:shoot ratio (**Supplementary Tables 4** and **5**), which suggests that it might increase root lodging in the field. We scored this attribute in the Ag Eq trials and noted no differences between transgenics and controls (not shown). This trend was not observed in the water-deficit block. **Supplementary Tables 6** and **7** show that in the 2006 study total dry weight was higher for transgenics than for controls, except for event 5223, particularly in the well-watered block. The correlation matrices for 2006 data in show a strong positive relationship between kernel number, kernel weight, ear weight and harvest index (**Fig. 5**). These components showed a modest but highly significant (see **Supplementary Fig. 4**) negative correlation with shoot dry weight, providing evidence that shoots and ears are competing sinks. This relationship was evident, but weaker, in the well-watered block (**Fig. 5b**). The data showed that *OsMads6-Tpp1* has a strong tendency to increase kernel set, especially in the water-deficit treatment block (**Fig. 5a**). Analysis of variance (**Supplementary Table 8**) showed that kernel weight, total dry weight and harvest index overall differed significantly between transgenics and controls. Together with the field results, the data suggest that *OsMads6-Tpp1* improves kernel set by enabling more effective resource pull, possibly from stem reserves, consistent with breeding strategies to improve grain yield[56].

Expression control and yield benefit

The *OsMads13* expression cassette showed activity in similar tissues as *OsMads6*, including the ear vasculature and ear spikelets that were targeted for trait gene expression. It was less active at the base of the ear node (where it attaches to the stalk). The cassette was also much less active in the vasculature that extended into the ear and was slightly less prevalent in ear vasculature (**Supplementary Fig. 5**). It did have activity in cell files that may define vestigial florets. In rice *OsMads13* specifies ovules and is expressed only in ovules[57], whereas *OsMads6* specifies floral meristem identity and is more broadly expressed in developing flowers[48]. In 2006, transgenic events with *OsMads13-Tpp1* were examined for responses to water deficit at the LaSalle, Colorado, farm, but in a trial separate from the *OsMads6-Tpp1* events. *OsMads13-Tpp1* had a consistent detrimental effect on yield preservation (**Supplementary Table 9**). The data showed that the *OsMads13-Tpp1* trait negatively influenced yield preservation compared to that in controls, whereas *OsMads6-Tpp1* increased yield preservation. To our knowledge this is the first demonstration that trait gene expression control (where and when a trait gene is active) can contribute substantially to the performance of a water optimization trait in the field.

DISCUSSION

Crop yields must double in the next 35 years to meet projected global food demand[4,5]. This requirement is coincident with unprecedented climatic variability. Drought, particularly at flowering, limits agricultural productivity in most crops. In maize this accounts for 40% of yield losses[1,8]. Accordingly, addressing the problem of drought at flowering has been a priority for crop improvement. On the basis of earlier evidence, we hypothesized that drought perturbs sucrose metabolism in developing ear spikelets and leads to kernel abortion, and that increasing sucrose supply to ear spikelets or altering sucrose

metabolism in young developing ears would improve kernel set in drought-prone environments[8,16]. Modification of T6P levels has been proposed as a means to achieve changes in sucrose metabolism[24]. Expression of a TPP gene with a floral MADS-box gene expression regulator increased ear spikelet sucrose content and kernel set, which increased harvest index and maize yield, under a range of water deficit conditions in addition to well-watered conditions in the field. This showed that maize's response to water deficit could be approached as a plant development problem, as there is only one opportunity to set yield in production environments.

The demonstration of the efficacy of drought-tolerant GM crops in the field has been extremely rare. This may be because a complex trait such as drought tolerance requires larger genetic changes than can be achieved through a target-gene approach and because the inherent variability and heterogeneity of the field environment makes it difficult to translate promising leads from laboratory to field. This report shows that a target-gene approach can work in the field. It remains to be seen whether this is a unique feature of the trehalose pathway or whether other single-gene manipulations can also produce such large effects. Nevertheless it is clear that trehalose metabolism exerts substantial control on yield in maize. This work provides a paradigm for the field evaluation of GM crops necessary for successful agricultural biotechnology product evaluation. We overcame the difficulties in demonstrating robust and reproducible yield data by conducting field trials throughout North and South America with GM lines grown alongside control plants and using a checkerboard plot layout. Trials were conducted in three successive years, using at least six or seven independent transgenic lines. Hybrids adapted to both short- and long-season environments were used as genetic backgrounds for trait evaluation and were cultivated in early- and late-maturity environments, respectively. Our work shows how the promise of fundamental plant biology can be taken from the laboratory to the field using a target-gene approach to deliver large yield increases.

Analysis of yield components in transgenics showed increased harvest index because of greater kernel set (**Table 1** and **Fig. 5**). Sucrose content in ear spikelets was also increased by about 20%, accompanying a two- to threefold decrease in T6P (**Fig. 2**). We put forward two possible explanations for the yield effect. First, T6P may alter sucrose metabolism within the ear spikelet. Amounts of S6P and G6P were 10% and 40% higher, respectively, in transgenic spikelets than in WT control spikelets under drought conditions **(Supplementary Fig. 2)**. In the absence of drought stress, however, G6P was lower in the transgenic spikelets than in the controls, and UDPG was lower in one transgenic event. These changes do not provide evidence for clear-cut metabolic effects in spikelets. Whatever the significance of these metabolic differences may be, sucrose was consistently higher in transgenic spikelets. Alternatively, it has been proposed that the T6P:sucrose ratio is a critical parameter for the plant and forms part of a mechanism to maintain sucrose levels within a range appropriate for cell type and developmental stage[58]. It is possible that changing this ratio with *OsMads6-Tpp1* enabled spikelets to receive more sucrose from the plant. Sucrose is required for spikelet development and may be the signal preventing starvation-induced abortion. SnRK1 activity in spikelets was inhibited by T6P, and changes in T6P levels in the transgenics were in the physiological range necessary for effects on *in vivo* SnRK1 activity (**Fig. 2c**,**d**). It is yet to be established whether T6P regulation of SnRK1 is sufficient to explain the yield effects seen here. Nevertheless, SnRK1 has been shown to affect whole-plant carbon allocation[59], consistent with altered sucrose allocation to spikelets. SnRK1 activities were decreased by drought similarly in all genotypes. This may be a natural response to drought that has not yet been genetically optimized for crop productivity. The selective large decrease of T6P in the transgenics would ensure greater *in vivo* SnRK1 activity in the transgenics compared to the controls (**Fig. 2c**,**d**). More work is necessary to understand the full complexity of all the factors influencing improved kernel set.

Trehalose levels did not differ between controls and transgenics, and trehalose may have no direct role in drought tolerance in maize and may only be relevant in resurrection plants[60,61]. *OsMads6-Tpp1* is not expressed in photosynthetic tissue, and we observed no clear changes in leaf photosynthesis in transgenics compared to controls (data not shown), although changes in total photosynthesis per plant cannot be ruled out. Additionally, altered allocation of assimilate from stems to ears could account for the yield increases as revealed in the correlation analyses of yield components (**Fig. 5**).

Our data suggest that TPP's capacity to prevent kernel abortion is cell specific. Histochemical localization of β-glucuronidase (GUS) showed very specific trait gene expression differences between *OsMads6* and *OsMads13* (**Fig. 1b** and **Supplementary Fig. 5**). It is notable that *OsMads13* was not successful in improving yield (**Supplementary Table 9**). This is entirely consistent with the strong regulation by T6P being dependent on cell location. TPP has highly cell-specific expression profiles[62], and our evidence suggests that not all cells are poised to use T6P as a metabolic control point to increase maize yield. To date, expression control has received very little attention, particularly for traits designed to alter plant responses to water deficit.

Over the past 15 years the trehalose pathway has come to be recognized as a central system of integrating growth and development with sucrose supply. Here we have shown how expression of a TPP gene can be targeted (driven by an *OsMads6* promoter) to alter T6P and improve harvest index and yield in the field. Extensive field trial data showed yield increases under all watering regimes typically experienced in North and South America for the world's highest yielding grain crop, maize. The T6P:sucrose ratio is a regulatory nexus in plants[58], and reducing T6P in ear spikelets positively influenced kernel set, particularly in plants exposed to water deficit. The approach of modifying T6P in specific sink tissues provides a novel and rational means of increasing crop performance. This technology forms the basis for further definitive product development, and its application to other cereals and crops could have a dramatic impact on global food security.

METHODS

Methods and any associated references are available in the online version of the paper.

Note: Any Supplementary Information and Source Data files are available in the online version of the paper.

ACKNOWLEDGMENTS

We thank E. Cates and M. Yarnall for technical assistance. L. Payan, C. Chaulk-Grace and L. Mansur managed the field trial locations. We also thank our Syngenta colleagues for their enthusiasm and support of this work. We thank M.-D. Chilton and the anonymous reviewers for helpful comments. Trehalose metabolite measurements were done by Metabolon. Rothamsted Research receives strategic funding from the Biotechnological and Biological Sciences Research Council of the U.K.

AUTHOR CONTRIBUTIONS

M.L.N. and L.M.L. conceived the study. M.L.N. designed the trait constructs and did the molecular characterization of the transgenic events. X.C. contributed to vector construction and event characterization. J.W. designed and conducted the greenhouse water deficit studies. H.-P.Z. and M.M. designed and managed the MSE and agronomic trials. Y.G. did the trait protein characterization. L.F.P. sampled for metabolite measurements, performed the SnRK1 assays and contributed to the histochemical analysis of the *OsMads6* expression cassette. S.S.B. and E.H. performed the metabolite analysis. R.M. did the statistical analysis. M.L.N. and M.J.P. wrote the paper.

COMPETING FINANCIAL INTERESTS
The authors declare competing financial interests: details are available in the online version of the paper.

1. Boyer, J.S. Plant productivity and environment. *Science* **218**, 443–448 (1982).
2. Araus, J., Slafer, G., Reynolds, M. & Royo, C. Plant breeding and drought in C3 cereals: what should we breed for? *Ann. Bot. (Lond.)* **89**, 925–940 (2002).
3. Elliott, J. *et al.* Predicting agricultural impacts of large-scale drought: 2012 and the case for better modeling. RDCEP Working Paper no. 13-01 (Grantham Research Institute on Climate Change and the Environment, 2013).
4. Ray, D.K., Mueller, N.D., West, P.C. & Foley, J.A. Yield trends are insufficient to double global crop production by 2050. *PLoS ONE* **8**, e66428 (2013).
5. Grassini, P., Eskridge, K.M. & Cassman, K.G. Distinguishing between yield advances and yield plateaus in historical crop production trends. *Nat. Commun.* **4**, 2918 (2013).
6. Cattivelli, L. *et al.* Drought tolerance improvement in crop plants: an integrated view from breeding to genomics. *Field Crops Res.* **105**, 1–14 (2008).
7. Araus, J.L., Serret, M.D. & Edmeades, G.O. Phenotyping maize for adaptation to drought. *Front. Physiol.* **3**, 1–20 (2012).
8. Boyer, J.S. & Westgate, M.E. Grain yields with limited water. *J. Exp. Bot.* **55**, 2385–2394 (2004).
9. Schussler, J.R. & Westgate, M.E. Maize kernel set at low water potential: II. sensitivity to reduced assimilates at pollination. *Crop Sci.* **31**, 1196–1203 (1991).
10. Schussler, J.R. & Westgate, M.E. Maize kernel set at low water potential: I. sensitivity to reduced assimilates during early kernel growth. *Crop Sci.* **31**, 1189–1195 (1991).
11. Kim, J.-Y., Mahe, A., Brangeon, J. & Prioul, J.-L. A maize vacuolar invertase, *IVR2*, is induced by water stress. Organ/tissue specificity and diurnal modulation of expression. *Plant Physiol.* **124**, 71–84 (2000).
12. Pelleschi, S., Rocher, J.-P. & Prioul, J.-L. Effect of water restriction on carbohydrate metabolism and photosynthesis in mature maize leaves. *Plant Cell Environ.* **20**, 493–503 (1997).
13. Saini, H.S. & Westgate, M.E. Reproductive development in grain crops during drought. *Adv. Agron.* **68**, 59–96 (1999).
14. Schussler, J.R. & Westgate, M.E. Assimilate flux determines kernel set at low water potential in maize. *Crop Sci.* **35**, 1074–1080 (1995).
15. Zinselmeier, C., Westgate, M.E., Schussler, J.R. & Jones, R.J. Low water potential disrupts carbohydrate metabolism in maize (*Zea mays* L.) ovaries. *Plant Physiol.* **107**, 385–391 (1995).
16. Zinselmeier, C., Lauer, M.J. & Boyer, J.S. Reversing drought-induced losses in grain yield: sucrose maintains embryo growth in maize. *Crop Sci.* **35**, 1390–1400 (1995).
17. Ruan, Y.-L., Jin, Y., Yang, Y.-J., Li, G.-J. & Boyer, J.S. Sugar input, metabolism and signaling mediated by invertase: roles in development, yield potential and response to drought and heat. *Mol. Plant* **3**, 942–955 (2010).
18. Boyer, J.S. & McLaughlin, J.E. Functional reversion to identify controlling genes in multigenic responses: analysis of floral abortion. *J. Exp. Bot.* **58**, 267–277 (2007).
19. Campos, H., Cooper, M., Habben, J.E., Edmeades, G.O. & Schussler, J.R. Improving drought tolerance in maize: a view from industry. *Field Crops Res.* **90**, 19–34 (2004).
20. Xiao, B.Z. *et al.* Evaluation of seven function-known candidate genes for their effects on improving drought resistance of transgenic rice under field conditions. *Mol. Plant* **2**, 73–83 (2009).
21. Nelson, D.E. *et al.* Plant nuclear factor Y (NF-Y) B subunits confer drought tolerance and lead to improved corn yields on water-limited acres. *Proc. Natl. Acad. Sci. USA* **104**, 16450–16455 (2007).
22. Castiglioni, P. *et al.* Bacterial RNA chaperones confer abiotic stress tolerance in plants and improved grain yield in maize under water-limited conditions. *Plant Physiol.* **147**, 446–455 (2008).
23. Virlouvet, L. *et al.* The ZmASR1 protein influences branched-chain amino acid biosynthesis and maintains kernel yield in maize under water-limited conditions. *Plant Physiol.* **157**, 917–936 (2011).
24. Habben, J.E. *et al.* Transgenic alteration of ethylene biosynthesis increases grain yield in maize under field drought-stress conditions. *Plant Biotechnol. J.* **12**, 685–693 (2014).
25. Morsy, M. Microbial symbionts: a potential bio-boom. *J. Investig. Genomics* **2**, 00015 (2015).
26. Paul, M.J., Primavesi, L.F., Jhurreea, D.J. & Zhang, Y. Trehalose metabolism and signaling. *Annu. Rev. Plant Biol.* **59**, 417–441 (2008).
27. Nunes, C. *et al.* The trehalose 6-phosphate/SnRK1 signaling pathway primes growth recovery following relief of sink limitation. *Plant Physiol.* **162**, 1720–1732 (2013).
28. Schluepmann, H., Pellny, T., van Dijken, A., Smeekens, S. & Paul, M. Trehalose 6-phosphate is indispensible for carbohydrate utilization and growth in *Arabidopsis thaliana*. *Proc. Natl. Acad. Sci. USA* **100**, 6849–6854 (2003).
29. Zhang, Y. *et al.* Inhibition of SNF1-related protein kinase1 activity and regulation of metabolic pathways by trehalose-6-phosphate. *Plant Physiol.* **149**, 1860–1871 (2009).
30. Martinez-Barajas, E. *et al.* Wheat grain development is characterized by remarkable trehalose-6-phosphate accumulation pre-grain filling: tissue distribution and relationship to SNF1-related protein kinase1 activity. *Plant Physiol.* **156**, 373–381 (2011).
31. Nunes, C. *et al.* Inhibition of SnRK1 by metabolites: tissue-dependent effects and cooperative inhibition by glucose-1-phosphate in combination with trehalose-6-phosphate. *Plant Physiol. Biochem.* **63**, 89–98 (2013).
32. Paul, M.J. *et al.* Upregulation of biosynthetic processes associated with growth by trehalose 6-phosphate. *Plant Signal. Behav.* **5**, 386–392 (2010).
33. Schluepmann, H., Berke, L. & Sanchez-Perez, G.F. Metabolism control over growth: a case for trehalose-6-phosphate in plants. *J. Exp. Bot.* **63**, 3379–3390 (2012).
34. Satoh-Nagasawa, N., Nagasawa, N., Malcomber, S., Sakai, H. & Jackson, D. A trehalose metabolic enzyme controls inflorescence architecture in maize. *Nature* **441**, 227–230 (2006).
35. Pilon-Smits, E.A.H. *et al.* Improved performance of transgenic fructan-accumulating tobacco under drought stress. *Plant Physiol.* **107**, 125–130 (1995).
36. Holmstrom, K.-O., Mantyla, E., Welin, B., Mandal, A. & Palva, E.T. Drought tolerance in tobacco. *Nature* **379**, 683–684 (1996).
37. Romero, C., Belles, J.M., Vaya, J.L., Serrano, R. & Culianez-Macia, F.A. Expression of the yeast trehalose-6-phosphate synthase gene in transgenic tobacco plants: pleiotropic phenotypes include drought tolerance. *Planta* **201**, 293–297 (1997).
38. Lee, S.-B. *et al.* Accumulation of trehalose within transgenic chloroplasts confers drought tolerance. *Mol. Breed.* **11**, 1–13 (2003).
39. Karim, S. *et al.* Improved drought tolerance without undesired side effects in transgenic plants producing trehalose. *Plant Mol. Biol.* **64**, 371–386 (2007).
40. Miranda, J.A. *et al.* A bifunctional TPS-TPP enzyme from yeast confers tolerance to multiple and extreme abiotic-stress conditions in transgenic *Arabidopsis*. *Planta* **226**, 1411–1421 (2007).
41. Van Houtte, H., Lopez-Galvis, L., Vandesteene, L., Beeckman, T. & Van Dijck, P. Redundant and non-redundant roles of the trehalose-6-phosphate phosphatases in leaf growth, root hair specification and energy-responses in *Arabidopsis*. *Plant Signal. Behav.* **8**, e23209 (2013).
42. Garg, A.K. *et al.* Trehalose accumulation in rice plants confers high tolerance levels to different abiotic stresses. *Proc. Natl. Acad. Sci. USA* **99**, 15898–15903 (2002).
43. Jang, I.-C. *et al.* Expression of a bifunctional fusion of the *Escherichia coli* genes for trehalose-6-phosphate synthase and trehalose-6-phosphate phosphatase in transgenic rice plants increases trehalose accumulation and abiotic stress tolerance without stunting growth. *Plant Physiol.* **131**, 516–524 (2003).
44. Li, H.-W., Zang, B.-S., Deng, X.-W. & Wang, X.-P. Overexpression of the trehalose-6-phosphate synthase gene *OsTPS1* enhances abiotic stress tolerance in rice. *Planta* **234**, 1007–1018 (2011).
45. Yeo, E.-T. *et al.* Genetic engineering of drought resistant potato plants by introduction of the trehalose-6-phosphate synthase (*TPS1*) gene from *Saccharomyces cerevisiae*. *Mol. Cells* **10**, 263–268 (2000).
46. Cortina, C. & Culiáñez-Macià, F.A. Tomato abiotic stress enhanced tolerance by trehalose biosynthesis. *Plant Sci.* **169**, 75–82 (2005).
47. Arora, R. *et al.* MADS-box gene family in rice: genome-wide identification, organization and expression profiling during reproductive development and stress. *BMC Genomics* **8**, 242 (2007).
48. Li, H. *et al.* The AGL6-line gene *OsMADS6* regulates floral organ and meristem identities in rice. *Cell Res.* **20**, 299–313 (2010).
49. Zhang, J., Nallamilli, B.R., Mujahid, H. & Peng, Z. *OsMADS6* plays an essential role in endosperm nutrient accumulation and is subject to epigenetic regulation in rice (*Oryza sativa*). *Plant J.* **64**, 604–617 (2010).
50. Pramanik, M.H.R. & Imai, R. Functional identification of a trehalose-6-phosphate phosphatase gene that is involved in transient induction of trehalose biosynthesis during chilling stress in rice. *Plant Mol. Biol.* **58**, 751–762 (2005).
51. Shima, S., Matsui, H., Tahara, S. & Imai, R. Biochemical characterization of rice trehalose-6-phosphate phosphatases supports distinctive functions of these plant enzymes. *FEBS J.* **274**, 1192–1201 (2007).
52. Nuccio, M.L., Chen, X., Conville, J., Zhou, A. & Liu, X. in *Recent Advances in Gene Expression and Enabling Technology in Crop Plants* (eds. Azhakanandam, K., Silverstone, A., Daniell, H. & Davey, M.) 41–78 (Springer, New York, Heidelberg, Dordrecht, London, 2015).
53. Barker, T. *et al.* Improving drought tolerance in maize. *Plant Breed. Rev.* **25**, 173–253 (2005).
54. Masuka, B., Araus, J.L., Das, B., Sonder, K. & Cairns, J.E. Phenotyping for abiotic stress tolerance in maize. *J. Integr. Plant Biol.* **54**, 238–249 (2012).
55. Snedecor, G.W. & Cochran, W.G. *Statistical Methods* 8th edn. (Iowa State University Press, Ames, Iowa, USA, 1989).
56. Richards, R.A. Selectable traits to increase crop photosynthesis and yield of grain crops. *J. Exp. Bot.* **51**, 447–458 (2000).
57. Dreni, L. *et al.* The D-lineage MADS-box gene *OsMADS13* controls ovule identity in rice. *Plant J.* **52**, 690–699 (2007).
58. Yadav, U.P. *et al.* The sucrose-trehalose 6-phosphate (Tre6P) nexus: specificity and mechanisms of sucrose signalling by Tre6P. *J. Exp. Bot.* **65**, 1051–1068 (2014).
59. Schwachtje, J. *et al.* SNF1-related kinases allow plants to tolerate herbivory by allocating carbon to roots. *Proc. Natl. Acad. Sci. USA* **103**, 12935–12940 (2006).
60. Bianchi, G. *et al.* The unusual sugar composition in leaves of the resurrection plant *Myrothamnus flabellifolia*. *Physiol. Plant.* **87**, 223–226 (1993).
61. Bartels, D. & Salamini, F. Dessication tolerance in the resurrection plant *Craterostigma plantagineum*. A contribution to the study of drought tolerance at the molecular level. *Plant Physiol.* **127**, 1346–1353 (2001).
62. Schluepmann, H. & Paul, M. Trehalose metabolites in *Arabidopsis*—elusive, active and central. *Arabidopsis Book* 7 e0122 (2009).

ONLINE METHODS

Vector construction and plant transformation. The DNA sequences encoding OsMADS6 (ref. 63) and OsMADS13 (ref. 64) were identified in a draft rice genome database[65] by BLASTP[66] using the DoMADS3 (ref. 67) protein as the query sequence. BLASTN[66] queries with Os*MADS6* (GenBank accession: U78782) identified two ESTs, CA760362 and CA766050, and one genomic DNA (gDNA) contig, Syngenta clone ID CLB6133.4. The *OsMads13* cDNA sequence (GenBank accession: AF151693) was used to identify its corresponding gDNA sequence in the rice genome database[65] (Syngenta clone ID CL004886.208). The cDNAs were used to annotate the gDNAs to define introns, exons, transcribed but untranslated sequences (UTRs) and flanking regulatory sequences and to localize the translation start and stop codons. The gDNAs precisely represent the cDNAs and 'GT…AG' border sequence flanks each intron.

To construct the GUS assembly vector, the *GUS* coding sequence, which includes an engineered intron, was amplified from pNOV5003 (Syngenta Crop Protection, LLC) in a Pfu Turbo polymerase (Stratagene, Cat. No. 600250) reaction. The reaction mixture consisted of 1 µL pNOV5003 miniprep DNA (prepared using the QIAprep Spin Miniprep procedure from Qiagen, Cat. No. 27106), 200 µM dNTP mixture (dATP, dCTP, dGTP, TTP), 1 µL 20 µM GUS5 oligonucleotide primer (5′-ATGGTACGTCCTGTAGAAACC-3′), 1 µL 20 µM GUS3 oligonucleotide primer (5′-GATCGAGCTCTCATTGTTT GCCTCCCTG-3′), 5 µL 10× cloned Pfu buffer and 2.5 units of Pfu Turbo DNA polymerase in a final volume of 50 µL. The thermocycling program was 95 °C for 30 s, 10 cycles of (95 °C for 5 s, 55 °C for 10 s, 72 °C for 2.5 min), 20 cycles of (95 °C for 5 s, 57 °C for 15 s, 72 °C for 2.5 min) and 72 °C for 2.5 min. The 2.2-kb *GUS* PCR product was gel purified, and ligated with pSP73 (Promega, Cat. No. P2221) digested with SmaI-SacI as a SacI fragment using the Takara DNA Ligation Mix, Version II (Cat. No. TAK 6022). The reaction was incubated at 16 °C for 30 min, and 7.5 µL of ligation mix was transformed into 50 µL XL-1 supercompetent cells (Stratagene, Cat. No. 200236) following the manufacturer's instructions. The pSP73-GUS recombinants were verified by digesting miniprep DNA with XbaI and SacI. Additional restriction sites were added to the pSP73-GUS polylinker to increase flexibility at the 3′-terminus of the *GUS* coding sequence by ligating a synthetic adaptor to the vector. The adaptor (Synthetic Adaptor I) was made by combining 40 µL of 50 µM oligonucleotide PL-F (5′-pCCGCGGGCGGCCGCACTAGTCCCGGGCCCAT-3′), 40 µL of 50 µM oligonucleotide PL-R (5′-pCGATGGGCCCGGGACTAGTG CGGCCGCCCGCGGAGCT-3′) (where 'p' is a 5′-phosphate group) in a 100 µL mixture that is 25 mM Tris-HCl (pH 8.0) and 10 mM $MgCl_2$. The mixture was boiled for 5 min, removed from heat and naturally cooled to room temperature (about 60 min). This yielded a 20 µM Synthetic Adaptor I solution. The pSP73-GUS construct was digested with SacI and ClaI, treated with calf-intestinal alkaline phosphatase (CIP, New England Biolabs, Cat. No. M0290S) and resolved on a 1% TAE agarose gel. The pSP73-GUS (digested with SacI and ClaI, and CIP-treated) DNA band was excised, recovered using the QIAquick Gel extraction kit (Qiagen, Cat. No. 28704) and precipitated with 20 µg glycogen, 0.3 M sodium acetate (pH 5.2) and 2.5 volumes ethanol at –20 °C for more than 2 h. The DNA was recovered by microcentrifugation, washed with 70% ethanol, dried under vacuum, resuspended in 5 µL ddH_2O and ligated to Synthetic Adaptor I. The pSP73-GUS-mod recombinants were verified by NotI digestion. The finished vector was designated pNOV6901.

The *Agrobacterium* binary vector was made to facilitate mobilization of expression cassettes constructed in pNOV6901 into plants. The pNOV2115 vector (Syngenta Crop Protection, LLC) was modified by inserting an adaptor that introduces the PacI, SgFI and RsrII restriction endonuclease recognition sites. The vector was digested with KpnI and HindIII, treated with CIP, gel purified and ligated to Synthetic Adaptor II. Synthetic Adaptor II was made by combining the oligonucleotides PL1 (5′-pGTACCGGACCGCGATCGCTT AATTA-3′) and PL2 (5′-pAGCTTAATTAAGCGATCGCGGTCCG-3′) where 'p' is a 5′-phosphate group. The pNOV2115-mod recombinants were verified by restriction analysis using KpnI, HindIII, PacI and RsrII. The vector was designated pNOV6900.

High-fidelity PCR was used to amplify the 4.5-kb *OsMads6* 5′-regulatory sequence from rice gDNA template using primers OsMADS#6-P1 (5′-CTA GGACGATGGTGTGATGTGGGAACACG-3′) and OsMADS#6-P2 (5′-GT ACCTTTCTAAAGTCTTTGTTATGCTGCAC-3′) and this was cloned using the TOPO XL PCR cloning kit (Invitrogen, Cat. No. K4750-20) following the manufacturer's instructions. The recombinants were identified by EcoRI digestion. The *OsMads6* promoter was made in several steps. The 3′ half (OsMADS-6Pb, about 2.96 kb) was produced by high-fidelity PCR from the *OsMads6* 5′-gene regulatory sequence clone using the OsMADS6-P3b (5′-CGAGTCG ACGAGGGGAAGAGTTGAGCTGAG -3′), and OsMADS6-P4c (5′-GACTC CATGGTGGTTATGCTGCACAAAAATG-3′) primers and cloned with the Zero Blunt TOPO PCR cloning kit (Invitrogen, Cat. No. K2875-20) following the manufacturer's instructions. Recombinants were verified by EcoRI digestion. The 5′ half (OsMADS-6Pa, about 1.5 kb) was produced by high-fidelity PCR from the pCR-XL-TOPO-OsMADS6-5′-gDNA clone using OsMADS6-C1b (5′-CAGTGCATGCGGACCGCTAGGACGATGGTGTGATGTG-3′), and OsMADS6-Paa (5′-CCTCGTCGACTCGCCCGATCGATCGAACG-3′) primers and cloned into the pCR-Blunt-II-TOPO vector. Recombinants were verified by EcoRI digestion. The 2.96-kb OsMADS6-Pb SalI-NcoI DNA fragment and the 1.5-kb OsMADS6-Pa SalI-SphI DNA fragment were sequentially ligated to pNOV6901.

High-fidelity PCR was used to amplify the *OsMads6* 3′-regulatory sequence from rice genomic DNA (gDNA) and the primers OsMADS#6-T1 (5′-GCTAAG CAGCCATCGATCAGCTGTCAG-3′) OsMADS#6-T2 (5′-GATGCCATTGTG TAATGAATGGAGGAGAGC-3′). The 1.2-kb DNA product was TOPO-cloned and a positive recombinant was identified by EcoRI digestion. The ~1.3-kb *OsMads6* 3′-regulatory sequence for the expression cassette was produced by high-fidelity PCR from the pCR-II-Blunt-OsMADS6-3′-gDNA clone using the OsMADS6-C4b (5′-ACGTGAGCTCGCTAAGCAGCCATCGATCAG-3′) and OsMADS6-C2 (5′-ACTGCGGACCGATGCCATTGTGTAATGAATGG-3′) primers. The 1.3-kb product was ligated to pNOV6901-OsMADS6P as a SmaI fragment. Positive pNOV6901-OsMADS6P-OsMADS6T recombinants were verified by digesting with RsrII. The plasmid was designated 11082 and contains the *OsMads6-GUS* expression cassette. The *OsMads6-GUS* expression cassette was ligated to pNOV6900 as an RsrII fragment to create the 11083 binary vector.

High-fidelity PCR was used to amplify the *OsMads13* 5′-regulatory sequence from rice genomic DNA (gDNA) using the OsMADS13-C1 (5′-GACTGCAGCGGACCGTTCCAAAATTAAGCACACACATTTG-3′) and (5′-GACTCCATGGCTTCTTGCTCTCAACTGATCAAC-3′) primers. The 1.9-kb product was ligated to pNOV6901 (SphI-blunt and NcoI-digested) as an NcoI fragment. Positive pNOV6901-OsMADS13P recombinants were verified by digesting with XhoI and NcoI. High-fidelity PCR was used to amplify the *OsMads13* 3′-regulatory sequence from rice genomic DNA (gDNA) with the OsMADS13-C3 (5′-TCGAGCGGCCGCTGACATGGATATGATGATCAG-3′) and OsMADS13-C4 (5′-ACGTATCGATCGGACCGCAACGCACGGGCACC CAAC-3′) primers. The 1.2-kb OsMADS13-3′-gDNA fragment was ligated to pNOV6901-OsMADS13P (digested with SmaI and NotI) as a NotI fragment. Positive pNOV6901-OsMADS13P/OsMADS13T recombinants were verified by NotI digestion. This produced the vector pNOV6904 which contains the *OsMads13-GUS* expression cassette. *OsMads13-GUS* was ligated to pNOV6900 as an RsrII fragment. This binary vector was designated pNOV6905.

The *Arabidopsis* genes At*TPPA* and At*TPPB* (GenBank accessions AF007778 and AF007779) which encode TPP enzymes with trehalose-6-phosphate phosphatase activity[68] were used in TBLASTN[66] queries of rice sequence databases. ESTs AU166371 and D15761 were the best hits and mapped to the same gDNA contig (Syngenta clone ID CI035214.105). The missing cDNA sequence was PCR amplified from a rice cDNA library with the oligonucleotide primers T6PP-F1 (5′-CAAAGCAGTGATGTCTCCCGTGATGAGAG-3′) and T6PP-R3 (5′-CAGATGGATCTCTCAGCGAGTAGAAGGC-3′) and the 696-bp product was TOPO cloned and sequenced. It precisely bridged the gap between the two ESTs, and alignment of the cDNAs to the *OsTpp1* gDNA defined the gene's coding sequence. The *OsTpp1* open reading frame was produced by high-fidelity PCR from a rice cDNA library, using the T6PP-EC-5 (5′-CATGGACCATGGATTTGAGCAATAGCTCAC-3′) and T6PP-EC-3 (5′-ATCGCAGAGCTCACACTGAGTGCTTCTTCC-3′) primers. The DNA product was TOPO-cloned and positive recombinants were verified by EcoRI digestion. To facilitate ligation into the *OsMads6* and *OsMads13* expression cassettes, an internal NcoI site in *OsTPP1* was silenced using Stratagene's QuikChange Multi Site-Directed Mutagenesis Kit (Catalog # 200514) and the oligonucleotide primer T6PP-QC (5′-CTTTATTATGCTGGAAGTCAT GGTATGGACATAATGGCACC-3′) following manufacturer's instructions.

doi:10.1038/nbt.3277

The *OsTpp1* coding sequence was excised as an NcoI-EcoICRI fragment and ligated to 11082 (NcoI-EcoICRI–digested) yielding the *OsMads6-Tpp1* expression cassette and pNOV6904 yielding the *OsMads13-Tpp1* expression cassette. Both cassettes were mobilized to pNOV6900 as RsrII fragments yielding binary vectors 12194 and 12212. All PCR products and DNA ligation junctions were verified by sequence analysis using the ABI PRISM dye terminator cycle sequencing kit (Perkin Elmer).

The *OsMads6-GUS*, *OsMads13-GUS*, *OsMads6-Tpp1* and *OsMads13-Tpp1* expression cassettes were inserted into the maize A188 inbred by *Agrobacterium*-mediated transformation[69]. T-DNA insertion was confirmed by primary and secondary TaqMan analysis[70] using several target assays that span the T-DNA insert and the binary vector backbone. Events lacking a vector backbone signal were retained. RT-PCR using T0 tassel florets and primers that flank the *OsMADS6-GUS* and *OsMADS13-GUS* expression cassette introns confirmed that both introns are correctly excised (not shown). RT-PCR was used to confirm transcription from the *OsMads6-Tpp1* and *OsMads13-Tpp1* trait genes. The RT-PCR primers used for *OsMads6-Tpp1* events were TPP-RTPCRF (5′-GACAGAACTGACGAAGACGCTTTCAAG-3′) and 6906-tr (5′-CTCCAACTTCTGACAGCTG-3′) and for *OsMads13-Tpp1* events were TPP-RTPCRF and 6904-tr (5′-AAAATGCAGCAGCACACAAATACTATA-3′). Unspliced RNA transcripts were not detected in any transgenic event. A representative PCR product was TOPO cloned and sequenced to verify the splice junction. The integrity of the TPP1 and phosphomannose isomerase (PMI) protein coding sequences in events 5217 and 5224 was confirmed as identical to the transformation vector sequence (not shown).

Western blot analysis. Enzymatically active recombinant TPP1 protein was prepared and processed as described[50]. The recombinant protein was used to produce goat polyclonal antiserum. A unique trait TPP1 peptide (LDAMKSS SPRRRLNVAFGEDNSSEE) was generated and coupled to an agarose column. The column was used to affinity purify antibodies that reacted specifically with the trait TPP1 protein. This was necessary due to crossreactivity with an endogenous signal that comigrated with the trait TPP1 protein. Ear spikelets from homozygous plants were harvested just before silk emergence and pulverized in liquid nitrogen. The powder was solubilized directly in SDS-PAGE sample buffer at 100 °C for 20 min. Extracted protein was clarified and quantified using the RC DC Protein Assay Kit (Bio-Rad, Cat. No. 500-0122). Extracts were resolved on 8–16% SDS-PAGE and transferred to PVDF membrane. The blot was developed using the affinity-purified goat–anti-OsTPP1 (2 µg/mL, or about 1:160 of the 0.318 mg/mL stock) followed by donkey–anti-goat-AP at a 1:5,000 dilution (Jackson ImmunoResearch Laboratories, Cat. No. 705-055-147). Color was developed by the addition of BCIP-NBT substrate (Moss, Inc., Cat. No. NBTM-100).

Assay for SnRK1 activity. Total soluble protein was extracted using a pestle and mortar from 200 mg of tissue ground under liquid nitrogen in 600 µL of ice-cold homogenization buffer of 100 mM Tricine-NaOH pH 8, 25 mM NaF, 5 mM dithiothreitol, 2 mM tetrasodium pyrophosphate, 0.5 mM EDTA, 0.5 mM EGTA, 1 mM benzamidine, 1 mM phenylmethylsulfonyl fluoride, 1 mM protease inhibitor cocktail (Sigma-Aldrich P9599), phosphatase inhibitors (PhosStop; Roche) and insoluble polyvinylpyrrolidone to 2% (wt/vol). Homogenate was centrifuged at 13,000*g* at 4 °C. Supernatant (250 µL) was desalted in illustra NAP-5 columns (GE Healthcare, Cat. No. 17-0853-02) pre-equilibrated with homogenization buffer. Eluant was supplemented with protease inhibitor cocktail and okadaic acid to 2.5 mM before freezing in liquid nitrogen. SnRK1 activity of three replicates for each time point was determined as described[29] in a final volume of 25 µL in microtiter plate wells at 30 °C. Assay medium was 40 mM HEPES-NaOH, pH 7.5, 5 mM $MgCl_2$, 200 mM ATP containing 12.5 kBq [γ-^{33}P]ATP (PerkinElmer), 200 µM AMARA peptide (Enzo Life Sciences, Cat. No. BML-P270-0001), 5 mM dithiothreitol, 1 µM okadaic acid and 1 mM protease inhibitor cocktail (Sigma-Aldrich, Cat. No. P9599). Assays were started with 5 µL extract and stopped after 6 min by transferring 15 µL to 4-cm^2 squares of Whatman P81 phosphocellulose paper and immersed immediately in 1% phosphoric acid. These were then washed with four 800-mL volumes of 1% phosphoric acid, immersed in acetone for 15 min, air dried and transferred to vials with 3.5 mL of Ultima Gold scintillation cocktail (Fisher, Cat. No. 50-905-0521).

Metabolite measurements. The transgenic and control plants were randomly arranged in the growth chamber and subjected to either drought-stress or unstressed conditions as they transitioned into reproductive development. Ear spikelets were harvested approximately 5 d before pollination and pooled before flash freezing in liquid nitrogen. Samples to measure metabolites consisted of tissue from four plants. Four samples were prepared from unstressed plants and five samples were prepared from drought-stressed plants. Samples were stored at –80 °C until extraction.

For sucrose, sugars soluble in 80% ethanol were extracted at room temperature (22 °C) from powdered floret tissue samples. Samples from WT control plants and two transgenic events, 5217 and 5224, were analyzed. Approximately 100 mg of tissue was weighed and vortexed in 500 µL 80% ethanol solution for 5 min at room temperature. Samples were then clarified by centrifugation at 15,700*g* for 10 min at room temperature in a bench-top centrifuge. The supernatants were collected, centrifuged again and then filtered through a MicroScreen-HV plate (Millipore, Cat. No. MAHVN4550). All filtered samples were diluted 50-fold with water before chromatographic analysis.

A Dionex ICS-3000 Ion Chromatography System equipped with a CarboPac PA1 column was used to resolve glucose, fructose and sucrose in each sample. Sugars were separated with a 35 min elution gradient (40 mM NaOH for 25 min, followed by a 0–300 mM sodium acetate gradient in 40 mM NaOH for 1 min, and then 40 mM NaOH for 9 min) at a flow rate of 1 mL/min. Sucrose, glucose and fructose were quantified by determining resolved peak areas using Chromeleon software and comparing to standard curves generated in the concentration range of 0.0125–0.2 mg/mL. Three measurements were done for each tissue sample and data are the mean ± standard error ($n = 4$).

Uridine-5′-diphosphoglucose (UDP-Glc)-$^{13}C_9$ was synthesized via an enzymatic reaction using uridine-5′-diphosphoglucose pyrophosphorylase (Sigma-Aldrich, Cat. No. U8501) with the substrates glucose-1-phosphate (G1P, Sigma-Aldrich, Cat. No. G6750) and $^{13}C_9$-labeled uridine-5′-triphosphate ([$^{13}C_9$]UTP, Sigma-Aldrich, Cat. No. G6750). 10 mg G1P, 5 mg [$^{13}C_9$]UTP, 25 units uridine-5′-diphosphoglucose pyrophosphorylase, and 100 units inorganic pyrophosphatase (Sigma-Aldrich, Cat. No. I1643) were mixed in 50 mM TRIZMA buffer pH 7.6 with 16 mM magnesium chloride (Sigma-Aldrich, Cat. No. M2670). Reaction progress was monitored by liquid chromatography coupled to tandem mass spectrometry (LC-MS/MS), and the reaction was quenched with methanol when no further progression was detected. Based on peak area comparison with an unlabeled UDPG standard, 1.4 mL of solution containing approximately 800 µg/mL UDPG[$^{13}C_9$] was obtained.

Trehalose-6-phosphate (T6P)-$^{13}C_{12}$ was synthesized via a water-mediated phosphorus oxychloride reaction with [$^{13}C_{12}$]trehalose (Omicron Biochemicals, Cat. No. TRE-002). [$^{13}C_{12}$]trehalose (100 mg) was added to 0.5 mL acetonitrile at 4 °C and mixed with phosphorus oxychloride (Sigma-Aldrich, Cat. No. 262099) and a small amount of water. The reaction was monitored by LC-MS/MS, which showed a mixture of products, including T6P[$^{13}C_{12}$]. The reaction was quenched with water when the maximum amount of T6P[$^{13}C_{12}$] was indicated. The resultant 1.5 mL of solution contained approximately 6.6 mg/mL T6P[$^{13}C_{12}$] based on peak area comparison with an unlabeled T6P standard.

Sucrose-6-phosphate (S6P)-$^{13}C_{12}$ was synthesized via a water-mediated phosphorus oxychloride reaction with [$^{13}C_{12}$]sucrose. [$^{13}C_{12}$]sucrose (100 mg) was added to 0.5 mL acetonitrile at 4 °C and mixed with phosphorus oxychloride and a small amount of water. The reaction was monitored by LC-MS/MS, which showed a mixture of products, including S6P[$^{13}C_{12}$]. The reaction was quenched with water when the maximum amount of S6P[$^{13}C_{12}$] was indicated. The resultant 5 mL of solution contained approximately 780 µg/mL of S6P[$^{13}C_{12}$] as estimated from peak area and comparison with an unlabeled S6P standard.

The internal standard solutions were mixed to obtain an internal standard working solution 1 containing UDPG[$^{13}C_9$] at 20 µg/mL, T6P[$^{13}C_{12}$] at 15 µg/mL, and S6P[$^{13}C_{12}$] at 25 µg/mL. 1 mg/ml stock solutions were separately prepared, in water, for G6P[$^{13}C_6$] and trehalose (Tre)-[$^{13}C_{12}$]. These two stock solutions were combined and diluted with methanol:water (80:20) to produce a working internal standard solution 2 containing G6P[$^{13}C_6$] at 50 µg/mL and Tre[$^{13}C_{12}$] at 20 µg/mL.

Powdered maize floret tissue sample (approximately 100 mg) was spiked with working ^{13}C-labeled internal standard solution, then homogenized and

extracted with methanol water (70:30). Homogenization and extraction of tissue samples was performed with a Genogrinder homogenization device. Following centrifugation, an aliquot of the clear supernatant was removed and injected onto an Agilent 1290/AB Sciex QTrap-5500 LC-MS-MS system equipped with an Acquity Amide UPLC column (Acquity BEH-Amide, 1.7 micron, 2.1 × 100 mm, Waters).

For estimation of T6P, S6P and UDPG, 2 µL (adjusted for sensitivity and linearity purposes) of sample with internal standard 1 was injected. Chromatography was carried out with 35% mobile phase A (200 mM ammonium bicarbonate in water) and 65% mobile phase B (acetonitrile) and isocratic flow at 0.800 mL/min.

Samples with internal standard solution 2 were used for estimation of G6P and trehalose contents. Chromatography through the Acquity Amide UPLC column was carried out with gradient flow at 0.40 mL/min for a total time of 7.0 min. Two mobile phases were: A, containing 200 mM ammonium formate with 0.5% ammonium hydroxide in water and B, containing 9:1 acetonitrile: methanol. The gradient used was: 0.0 min 5% mobile phase A and 95% mobile phase B; 3.9 min 28% mobile phase A and 72% mobile phase B; 4.4 min 50% mobile phase A and 50% mobile phase B; and 6.6 min 5% mobile phase A and 95% mobile phase B.

For maize floret tissue samples, the peak areas of the *m/z* 421.0→240.9 product ion of T6P, the *m/z* 421.0→240.9 product ion of S6P, the *m/z* 259.0→139.0, 169.0 and 199.0 product ions of G6P, the *m/z* 564.9→240.9 product ion of UDPG, and the *m/z* 341.2→59.0, 179.0, 89.1 and 119.0 product ions of trehalose were measured against the peak areas of the corresponding internal standard product ions of *m/z* 433.0→246.9, *m/z* 433.0→246.9, *m/z* 265.0→141.0, 172.0, and 203.0, *m/z* 573.9→240.9 and *m/z* 353.2→61.0, 185.0, 92.0 and 123.0.

The following LC-MS/MS methods were developed with a calibration range of 10.0 to 1,000 µg/g for G6P, 0.0500 to 50.0 µg/g for T6P, 0.500 to 500 µg/g for S6P, 0.500 to 500 µg/g for UDPG and 0.500 to 50.0 µg/g for trehalose. The peak areas of the T6P, S6P, G6P, UDPG and trehalose product ions were measured against the peak areas of the respective T6P[$^{13}C_{12}$], S6P[$^{13}C_{12}$], G6P[$^{13}C_6$], UDPG[$^{13}C_9$] and trehalose[$^{13}C_{12}$] internal standard product ions. Quantitation was performed using a weighted linear least-squares regression analysis generated from fortified calibration standards prepared immediately before analysis.

Statistical analysis was done for five composite samples for each genotype subjected to drought stress and for four composites from unstressed plants. Analysis of variance was done, and contrasts of each transgenic event with control plants (WT) were computed using Dunnett's procedure with JMP statistical software[71,72].

Field experiment trial design and statistical analysis. Field experiments were grown in randomized complete block design in the managed stress environments (MSE) in Visalia, CA, in 2004 and 2005, in LaSalle, CO, in 2005 and 2006, and in Los Andes, Chile, in 2005–2006. At these locations, water deficit experiments and well-watered experiments were grown (as treatments and replicates) with corn hybrids as blocks. Well-watered experiments had three replicates. Water deficit experiments had three replicates in CA 2004, 8–12 replicates in 2005, 9 replicates in CO 2005, 8–16 replicates in CO in 2006, and either 10 or 20 per entry in Chile 2005–2006. Event-positive hybrids for 5217, 5218 and 5224 each had 20 replicates, whereas 5220, 5221 and 5223 each had 10 replicates. If there was a null control selected for a transgenic (see field protocol below), it was placed immediately adjacent to the event-positive hybrid and randomly assigned to that pair of plots to improve accuracy of comparison. Multiple plots of the nontransformed control were also included in each replication in the water deficit experiments.

Statistical analyses for the MSE experiments were done using JMP statistical software[71,72]. Analyses of variance (ANOVA) for field trials used grain yield, number of barren plants per plot, and anthesis-silking interval (ASI) as dependent variables (*y* variables) and replication and hybrid as independent variables (*x* variables). A general linear model appropriate for the experimental design was used to generate the ANOVA table for each experiment. Planned contrasts of means of hybrid entries to their corresponding controls were done using single degree of freedom tests. Orthogonal comparisons provide independent tests of transgenic versus control for each hybrid (+, –) pair in the 2005 California and Chile field experiments. For the other three field experiments, Dunnett's procedure was used to control family-wise error rates in comparisons of each transgenic with its WT control.

A meta-analysis was done on the five MSE experiments and eight events whose results are shown in **Figure 3**. Hybrid yield means were analyzed using ANOVA with independent (*x*) variables: environment, event within environment and gene (positive or negative). Using hybrid means resulted in each hybrid within each environment being weighted equally in the analysis to avoid an overemphasis of some environments, e.g., the Chile 2005–2006 environment having 10–20 replicates. The contrast of the difference between the transgenic and control hybrid means was tested for statistical significance, and a 95% confidence interval was computed as $+0.50 \pm 0.17$ Mg ha^{-1} ($+8.0 \pm 2.7$ bushels acre^{-1}, $P < 0.0001$).

Agronomic equivalency field tests were grown in several locations in the Midwest of North America from 2004–2006 (**Supplementary Table 1**). Experiments were grown in randomized complete block design with three replicates for each location. Hybrid means were computed for each location and used in an analysis of variance with grain yield as dependent variable and location and hybrid as independent variables. Means of positive event hybrids are contrasted with their negative controls using Student's *t*-test.

Field protocol to evaluate yield preservation in maize exposed to water deficit. Hybrid seed were generated for each transgenic event at the Syngenta Seeds field stations in Kaua'i, HI, USA or Slater, IA, USA. T1 seed, obtained by selfing the T0 plant, of the events were sown in four single-row plots, 3.87 m long separated by 0.914 m alleys with about 20 plants per row. Taqman analysis[70] was used to divide the progeny into homozygous or hemizygous (containing the trait gene) and null (lost the trait gene) siblings. In two of the single-row plots, hemizygous and null plants were destroyed and homozygous plants were selfed for seed bulking and also test crossed as described in **Supplementary Table 1**. In the other two single-row plots homozygous and hemizygous plants were destroyed and null plants were selfed and test crossed as described in **Supplementary Table 1**. B1 seed were selfed before creating the test crosses. The null and hemizygous testcross seed of the events were used to conduct field trials.

Two field management protocols were used to evaluate transgene performance in plants exposed to a controlled water deficit. The Visalia, California, and Los Andes, Chile, locations used furrow irrigation to manage field water levels, and the LaSalle, Colorado, location used drip irrigation. Plot size was two 5.0 m rows with approximately 75-cm spacing between rows. There was a 60-cm alley between ranges. Forty seeds were planted in each row at a seeding rate of 8 seeds per meter and thinned to ~35 plants per row after emergence.

Standard cultivation procedures were followed to ensure a healthy crop. Herbicides, fungicides and pesticides were applied when necessary for optimal control of weeds, diseases and insects, respectively. Threats from animal damage were minimized. Fertilizers were applied as necessary.

Watermark soil moisture sensors were installed at 30-cm, 60-cm and 90-cm depths in multiple locations throughout the trial. Soil moisture probe data were recorded daily. Daily weather data were acquired either on site or from a nearby weather station (within 30 km) with similar climate environment as the trial site. Temperature, precipitation and evapotranspiration (ET) were recorded daily. Normal, optimal irrigation was applied to each trial using drip or furrow irrigation until approximately 30 d before flowering. Standard irrigation was every 3–4 days, applying 10–20 cm of water each time. The amount of water applied depended on the plant stage and weather conditions, with the objective to achieve uniform germination and a healthy stand.

The average of the 30-cm and 60-cm probes guided the irrigation schedule. Thirty days before projected flowering (50% pollen shed), the trials were irrigated to bring moisture in the top 3 feet of the soil profile to full capacity. Water was then withheld in the water deficit treatment until soil moisture was depleted to the target trigger point. Normal irrigation continued in the well watered treatment. The objective was to reach the target trigger point of 170 cBar at 7 d before flowering. If the soil probe average exceeded the trigger point by 10 cBar before the target trigger point, less than 10 mm of water was applied. From this point deficit irrigation at 30% ETc (the crop ET) using calculated ET and the crop coefficient was applied. Deficit irrigation was applied approximately every 4 d.

doi:10.1038/nbt.3277

Plants were monitored for stress symptoms (leaf curling or leaf firing) late in the afternoon. The time symptoms appeared was recorded each day. Depending on field conditions, the symptoms appeared an hour or two earlier each day, but plants recovered each morning and appeared as equally turgid as well watered plants. Deficit irrigation was continued until 14 d after flowering or when 90% of the plots reached silk emergence. Normal irrigation resumed by application of 150% daily ET for the next 2 irrigation cycles. This brought soil moisture to approximately 90% of water holding capacity.

During anthesis, the dates of 50% pollen shed and 50% silk emergence were recorded on a plot basis. The three end plants in each row were ignored due to border effects. Toward the end of the water deficit period, plots were rated for stress symptoms on a 1 to 9 scale (1 = turgid or no stress; 9 = severely stressed). Prior to harvest, the number of barren plants was recorded. A barren plant either had no ear or had an ear with no kernels. Harvest data were collected either manually or with a research combine (see **Supplementary Table 1**). For manual harvest, grain yield data were collected from the middle 4 m of each two-row plot and recorded as kg/plot. Percent grain moisture and test weight (a bulk density measurement, the weight of grain in a fixed volume) were also recorded.

Agronomic equivalency field tests. Hybrid seed was generated for each transgenic event as described above. A series of yield trials were conducted in several US Midwest locations to test transgene performance under conditions typically used by growers. The locations and testers are outlined in **Supplementary Table 1**. These populations also contained the *Bacillus thuringiensis* (*Bt*) transgene to control insect pressure. The experimental design consisted of randomized complete blocks with three replicates. Each experimental unit consisted of two-row plots, 5.33-m long planted with 34 kernels per row. Ranges were separated by 0.914-m alleys. For events for which there was seed of both the null and the hemizygous hybrids, randomization was restricted to keep the null and hemizygous hybrids of the events in neighboring plots. Most events were evaluated in eight or nine locations. Event 5224 was evaluated in three locations. After emergence, stand counts were taken and plots were thinned, as necessary, to establish field uniformity. During the growing season plots were evaluated for intactness, greensnap, root lodging, heat units to 50% pollen shed and heat units to 50% silk emergence. Plots were combine-harvested and grain yield and grain moisture were recorded. The data from hemizygous plots were compared to those from null plots, or to those from wild type plots where necessary, to gauge the transgene's effect on yield. Standard deviation (s.d.) for grain yield in this experiment was 15–20% of the mean. Growth conditions in the Midwest were ideal for maize in 2004. Depending on location, yields in this experiment averaged from 5.65–8.16 Mg ha^{-1} (90 to 130 bushels $acre^{-1}$).

Greenhouse water deficit experiments. Experiment design: Hybrid seed for each event was prepared at the Syngenta Kaua'i nursery as described above. Experiments were conducted in a greenhouse at the Syngenta Seeds facility in Slater, Iowa, USA. A minimum of 100 F1 seeds per event were planted in 5-cm (length) × 2.5-cm (width) × 5-cm (depth) cells to ensure that enough healthy plants were available for the study. One seed per cell was placed and covered with 3.8 cm of either coarse perlite or ground Q-Plug. Cells were watered once per day with misting sprayers or foggers. The greenhouse was maintained at 20–28 °C. Supplemental fluorescent lighting was provided 5 d after seeding from 06:00 to 20:00 daily.

When most plants had three visible leaf tips, seedlings were tested for presence of the trait gene using PMI AgraStrips (Romer Labs, Cat. No. 7000052). Trait-positive (transgenic) and null (control) plants for each event were paired when they had equal number of leaves and were similar in plant height. A minimum of 30 seedling pairs were selected for each event. Each pair was transplanted to 12.5-cm× 12.5-cm pots containing perlite or ground Q-Plug to the first leaf ligule. Pots were placed on gutters and bottom-watered by a thin film of water for 1 h per day. Hoagland's nutrient solution was applied once plants had four visible leaf-tips.

Seedlings were transplanted into tree pots at the seven leaf-tip stage. The pot growth medium was an isolite and turface mix. Two lengthwise rows, one for water deficit and one for normal irrigation, were set up and divided into three replicates from south to north. Within each replicate, there were eight plots with six plants each. The eight entries (genotypes) were randomly assigned to plots. The same randomization within each replication was used for water deficit and normal irrigation treatments. Thus, each row comprised a randomized complete block experiment, and together the water deficit and normal irrigation treatments comprised a split block without randomization of the water deficit– and normal-irrigation treatments. At least one generic hybrid pot was placed in the middle of each replication for ET measurement (ET-pots). The experimental plants were open pollenated and, to ensure adequate pollen availability, control plants were started a few days before and after the experimental plants.

Pots were drip-irrigated with Hoagland's solution six times a day (06:00–06:30, 08:00–08:30, 10:00–10:30, 12:00–12:30, 14:00–14:30 and 16:00–16:30). The nutrient solution tanks were replenished every other day. Just before reaching the 16 leaf-tip stage, plant irrigation was changed to three times per day (10:00–10:10, 12:00–12:10, 14:00–14:10) until the water deficit treatment. The water deficit treatment began when 50% of tassels in that block were visible from the leaf whorl. All plants were thoroughly irrigated before the treatments started. After excess water fully drained, the E-pots were weighed (W1). These pots received 0.5 l water each day until the day of supplemental watering (DSW; the date when 50% of plants reached a level 6.0 stress rating) and ET-pots were weighed again (W2). Level 6.0 stress is when all leaves are curled and the lower-most leaves show evidence of tip burn. ET was calculated according to the equation $ET = (0.5 \times n) + (W1 - W2)$, where n is the number of days elapsed from saturation to DSW.

The cycle was repeated by resaturating the ET-pots to determine ET. The water deficit treatment block received supplemental irrigation equivalent to 0.5× of ET. Treatment continued until the fourth DSW, or 10 d after the peak pollen-shed date, whichever came first. At the end of the water deficit treatment, all pots were saturated and returned to three irrigation cycles per day. Pollen shed and silk emergence dates for individual plants were recorded daily.

The 2005 greenhouse study consisted of three replicates per entry per treatment. Between three and six plants were harvested from each plot except for two control plots which had two plants harvested each. Data were averaged for each event and its corresponding check. Data collected included number of ear shoots, shoot and root dry weight, ear dry weight, kernel number, grain yield and biomass per plant, days to pollen shed after silk emergence and lastly plant height. The root to shoot ratio and harvest index were calculated from the data.

The 2006 greenhouse study consisted of four replicates for the water deficit and three replicates for the normal irrigation treatment. The hybrid background was FF6091 crossed to A188. Between three and six plants were harvested for each plot. Variables measured included days to silk emergence, kernel number, kernel weight (grain yield), ear dry weight, stem (shoot) dry weight and total dry weight. Harvest index was calculated from the data.

Statistical analysis of greenhouse experiments. ANOVA and correlation analyses were done with JMP statistical software[71,72]. The measured variables were considered dependent (y) variables and genotype and replicates were the independent (x) variables in the ANOVA. Differences between transgenic and control hybrids were tested for significance using single degree of freedom tests. Orthogonal comparisons provided independent tests of transgenic versus control for each hybrid (+, −) pair. Correlations among variables were computed using averages over individual plants for each hybrid within each replicate.

63. Moon, Y.-H., Jung, J.-Y., Kang, H.-G. & An, G. Identification of a rice *APETALA3* homologue by yeast two-hybrid screening. *Plant Mol. Biol.* **40**, 167–177 (1999).
64. Lopez-Dee, Z.P. *et al. OsMADS13*, a novel rice MADS-box gene expressed during ovule development. *Dev. Genet.* **25**, 237–244 (1999).
65. Goff, S.A. *et al.* A draft sequence of the rice genome (*Oryza sativa* L. ssp. japonica). *Science* **296**, 92–100 (2002).
66. Altschul, S.F. *et al.* Gapped BLAST and PSI-BLAST: a new generation of protein database search programs. *Nucleic Acids Res.* **25**, 3389–3402 (1997).
67. Yu, H. & Goh, C.J. Identification and characterization of three orchid MADS-box genes of the AP1/AGL9 subfamily during floral transition. *Plant Physiol.* **123**, 1325–1336 (2000).

68. Vogel, G., Aeschbacher, R.A., Muller, J., Boller, T. & Wiemben, A. Trehalose-6-phosphate phosphatases from *Arabidopsis thaliana*: identification by functional complementation of the yeast *tps2* mutant. *Plant J.* **13**, 673–683 (1998).
69. Negrotto, D., Jolley, M., Beer, S., Wenck, A.R. & Hansen, G. The use of phosphomannose-isomerase as a selectable marker to recover transgenic maize plants (*Zea mays* L.) via *Agrobacterium* transformation. *Plant Cell Rep.* **19**, 798–803 (2000).
70. Ingham, D.J., Beer, S., Money, S. & Hansen, G. Quantitative real-time PCR assay for determining copy number in transformed plants. *Biotechniques* **31**, 132–140 (2001).
71. Jones, B. & Sall, J. JMP statistical discovery software. *Wiley Interdiscip. Rev. Comput. Stat.* **3**, 188–194 (2011).
72. SAS Institute. *JMP 8 Statistics and Graphics Guide* 2nd edn. (SAS Institute, Inc., Cary, NC, USA, 2009).

doi:10.1038/nbt.3277